


CHANGES IN FOSSIL CO₂ EMISSIONS IN MEXICO CITY DURING THE COVID-19 LOCKDOWN DEDUCED FROM ATMOSPHERIC RADIOCARBON CONCENTRATIONS

Laura E Beramendi-Orosco^{1,2*}  • Galia González-Hernández^{1,3} • Edith Cienfuegos^{1,2} • Francisco Otero^{1,2}

¹Laboratorio Nacional de Geoquímica y Mineralogía – UNAM, Ciudad de México, 04510, México

²Instituto de Geología, Universidad Nacional Autónoma de México, Ciudad de México, 04510, México

³Instituto de Geofísica, Universidad Nacional Autónoma de México, Ciudad de México, 04510, México

ABSTRACT. We present atmospheric radiocarbon concentrations in CO₂ integrated samples taken between January 2019 and December 2021 in the Mexico City Metropolitan Area (MCMA) and explain the variations in terms of changes in emission sources associated with the COVID-19 lockdown restrictions imposed from March 2020. $\Delta^{14}\text{C}$ values for samples collected during 2019 range between -44.15‰ and -13.17‰ , with lower values during months with higher fossil fuels consumption and air stagnation, whereas higher values were found for periods with high number of fires around MCMA or wet months with higher contribution of heterotrophic respiration. For samples collected during 2020, $\Delta^{14}\text{C}$ values range between -17.7‰ and 2.25‰ , with an increasing trend immediately after the initial lockdown and higher values obtained for samples collected during lockdown phases 2 and 3 and the period of extremely high epidemic risk. This agrees with the 38% and 52% decrease in gasoline and diesel sales. Once essential activities gradually opened from July 2020, $\Delta^{14}\text{C}$ follow a decreasing trend as vehicle traffic started to increase again. $\Delta^{14}\text{C}$ values for samples collected during 2021 range from -32.89‰ to -10.27‰ , with the higher value obtained during a period of extremely high epidemic risk with a 30% reduction in gasoline and diesel consumption. Despite the complexity of emission sources in MCMA, from $\Delta^{14}\text{C}$ variations it was possible to identify changes in fossil CO₂ emissions resulting from the significant reduction in vehicle traffic due to the COVID-19 lockdown and the restrictions imposed to control transmission of the disease.

KEYWORDS: atmospheric radiocarbon, carbon dioxide emissions, COVID-19 lockdown, fossil CO₂, Mexico City.

INTRODUCTION

The Mexico City Metropolitan Area (MCMA) is a complex megacity with a mixture of CO₂ emission sources, where atmospheric radiocarbon (¹⁴C) variability is influenced mainly by changes in fossil fuel combustion and biomass burning from residential combustion, agricultural burning and wildfires in the mountains surrounding the valley, common during the dry season (winter and spring) (Beramendi-Orosco et al. 2015, 2018). Previous studies have reported $\Delta^{14}\text{C}$ levels in MCMA up to 75‰ and 27‰ higher than regional background values during the hot and dry season (Vay et al. 2009 and Beramendi-Orosco et al. 2015, respectively), attributed to the release of ¹⁴C-enriched CO₂ resulting from the burning of soil organic matter during agricultural and wild fires in the basin, suggesting this is a significant CO₂ emission source as it cancels out the ¹⁴C dilution resulting from the vast amount of fossil fuels burned this metropolitan area with high population density. These observations could result in an underestimation of the atmospheric fossil CO₂ concentration in the MCMA, hampering the direct use of ¹⁴C as a tracer of fossil CO₂ emissions in such a complex urban area (Beramendi-Orosco et al. 2018).

According to the latest published emissions inventory, in 2018 the MCMA emitted more than 66 million tons of CO₂, mainly from the transport sector (65.4%) with diesel and gasoline as the

*Corresponding author. Email: laurab@geologia.unam.mx



main fuels. Other important CO₂ sources are from the industrial sector, contributing with nearly 20% of the total emissions, and domestic combustion of natural gas, liquid propane gas and biomass, estimated to contribute up to 5.2%. Emissions from electricity generation and distribution accounts for 4.5% and the remaining 5% is attributed to other sources, including forest fires, landfills, and open combustion (SEDEMA 2021).

The greenhouse gases and other contaminants emitted within the MCMA are not easily dispersed because the basin is a closed valley surrounded by mountains and, depending on meteorological conditions, can result in air stagnation usually during the dry months (November–May), causing an increase in the concentration of air pollutants, mainly ozone and particulate matter (PM₁₀ and PM_{2.5}). The local environmental authority operates an atmospheric monitoring system (SIMAT) consisting of 24 automated monitoring stations distributed throughout the MCMA that analyse the concentration of CO, NO₂, O₃, SO₂, PM₁₀, and PM_{2.5} (criteria pollutants) on an hourly basis. When the concentration of a particular air pollutant surpasses an established air quality threshold depending on the pollutant, restrictions are imposed to industries and particular vehicles to reduce emissions until the pollutants concentration decrease again to acceptable levels. These restrictions usually last for one or two days depending also on changes of the meteorological conditions promoting ventilation of the valley. The SIMAT, however, does not include measurements of CO₂ concentration, making it difficult to identify changes in emission sources of this greenhouse gas and evaluate the effect of the actions taken to improve air quality and meet the reduction targets of greenhouse-gas emissions.

To stop the spread of the COVID-19 epidemic, the Mexican government imposed restrictions from March 2020, starting with a partial lockdown (phase 1) closing schools and universities on 20th of March 2020, extending to all non-essential activities with a significant reduction in private and public transport services on 31st of March (phase 2), and further restrictions with a complete lockdown imposed on 21st of April, when the country started the phase of higher risk of COVID-19 transmission (phase 3). This complete lockdown lasted up to 31st of May. From 1st of June some non-essential activities were gradually opened with some restrictions in place up to 2021, and schools and universities remaining closed up to September 2021 (Table 1). From this point, the government implemented a colour-coded system according to the epidemic risk level, with red indicating extremely high risk advising population to stay at home and imposing some restrictions in non-essential activities; orange for high epidemic risk with non-essential activities open only to 75% capacity; yellow to denote moderate risk with non-essential activities operating to 50% capacity, and green for low risk with no restrictions (Secretaría de Salud 2020). These social distancing measures for stopping the COVID-19 propagation, resulted in an important reduction of the urban activities, mainly reflected in traffic and public transport. The volume of fossil fuels sold by the national petroleum company, PEMEX, in the MCMA reflect these changes, with a decrease of 45%, 49% and 35% during April, May and June 2020, respectively, in comparison to the volume sold during the same months in 2019 (SENER, 2022). This is in accordance with the fact that 50% of the fossil fuels consumed in the MCMA are used by the transport sector (SEDEMA 2021).

A previous work reported an evaluation of the effect of the COVID-19 lockdown phases 2 and 3 on the concentration of criteria air pollutants in the MCMA (Hernández-Paniagua et al. 2021), finding that during phase 2 only NO₂ decreased significantly (between 10% and 23%), while O₃ increased up to 40%. During phase 3, NO₂, PM₁₀, and PM_{2.5} decreased by 43%, 20%,

Table 1 Chronology of COVID-19 lockdown phases and restrictions and in Mexico City Metropolitan Area. (Data from <https://www.gob.mx/salud/documentos/comunicados-tecnicos-diarios-COVID19>)

Date	Lockdown phase/ color of risk level	Restrictions /changes
20 March 2020	Phase 1	Schools and Universities closed.
31 March 2020	Phase 2	Stop of most non-essential activities with significant reduction in public transport.
21 April –31 May 2020	Phase 3	Complete lockdown, stop of all non-essential activities.
1 June 2020	Red	Restrictions according to color system in place. MCMA in color red with extended restrictions to non-essential activities.
29 June–20 Dec. 2020	Orange	Gradual activation of commercial sector restricted to 30% of capacity and short opening times.
21 Dec. 2020–14 Feb. 2021	Red	Restrictions to non-essential activities.
Feb 15–May 9	Orange	Gradual activation of commercial sector restricted to 50% of capacity and short opening times.
10 May–6 June	Yellow	Commercial and services sector open to 75% capacity.
7–20 June 2021	Green	Non-essential activities open with some restrictions on capacity and opening hours depending on activity. Schools open for on-site lessons.
21 June–25 July 2021	Yellow	Commercial and services sector open to 50% - 75% capacity depending on activity.
26 July–2 September 2021	Orange	Commercial and services sector open to 50% capacity. Schools closed for summer holidays.
3 September–17 October 2021	Yellow	Commercial and services sector open to 50% - 75% capacity depending on activity. Schools open for on-site activities.
From 18 October 2021	Green	No restrictions.

and 32%, respectively, and O₃ decreased in relation to phase 2, but did not show a significant decrease in comparison to the baseline.

To gain a better understanding of changes in CO₂ emissions in MCMA during the COVID-19 pandemic, we report atmospheric ¹⁴C concentrations from CO₂ monthly-integrated samples taken between January 2019–December 2021 at the southern area of the MCMA and explain the variations in terms of the COVID-19 lockdown phases and epidemic risk level.

METHODOLOGY

Study Area and Sampling Site

The MCMA has an area of 7866 km² located in a high-altitude (~2300 m.a.s.l.) closed basin surrounded by mountains, including the Popocatepetl active volcano located at 50 km southeast. According to the latest emissions inventory for the MCMA, in 2018 there were 21.69 million inhabitants, 6.3 million households, 6.01 million registered vehicles, and more than 1900 regulated industries, located mainly in the northwestern and central areas (SEDEMA 2021). About 64% of the area can be classified as urban whereas 34% correspond to conservation areas, including rural soils, forests, and shrublands, mainly located on the mountains to the South, East and West. The climate is tempered by altitude and influenced by tropical air masses during summer (May to October) and mid-latitude cold air masses from North America during winter (Jauregui 2004). The mean annual temperature is 16°C and the annual precipitation, concentrated in summer months, is 400–500 mm in the northern part of the basin and 700–1200 mm in the central and southern parts (Jauregui 2004; INEGI 2014).

The sampling point is located on the rooftop of a 3-story building inside the main campus of the Universidad Nacional Autónoma de México (UNAM), located at the southern end of the urban area of Mexico City (Figure 1). The campus comprises 700 Ha, of which about 237 Ha correspond to the “Pedregal de San Angel” ecological reserve. The campus is located over a basaltic substratum deposited during the eruption of the Xitle volcano. Vegetation at the reserve has a xerophilous scrubland aspect, with most species showing resistance to drought. Most plant species are herbaceous or shrubby, although it is also possible to find 7-m trees (Rzedowski and Rzedowski 2005; Castillo et al. 2007). Elsewhere, vegetation is dominated by introduced species in gardens and roads.

Sampling Procedure and ¹⁴C Analysis

Integrated samples were collected by pumping air (20 mL min⁻¹) through a column with 1 L of a 0.7M NaOH solution (carbonate-free, Sigma-Aldrich Mexico) for about 30 days during day-time only, at a height of 9 m from ground level at a well-ventilated point on the rooftop of the building housing the preparation laboratory. To avoid contamination with atmospheric CO₂ not corresponding to the sampling period, the NaOH solution was prepared in situ immediately before sampling started, and captured CO₃²⁻ was precipitated also in situ as BaCO₃ by adding an excess of BaCl₂ solution immediately after sampling stopped. The precipitated barium carbonate was recovered from solution within a few hours, washed with bi-distilled water, and dried at 50°C in the laboratory located on the ground floor of the building where sampling was performed. Once dried, samples were stored in sealed glass jars inside a vacuum desiccator before being sent for analysis.

Samples for the period January 2019–June 2021 were analyzed by accelerator mass spectrometry (AMS) at the Centro Nacional de Aceleradores (CNA), Seville, Spain. Prior to measurement, samples were graphitized using a Carbonate Handling system coupled to an AGE system. Analysis was performed using a MICADAS system. Samples for the period July–December 2021 were analyzed at the Keck Carbon Cycle AMS facility at University of California Irvine. All ¹⁴C results are reported as Δ¹⁴C corrected for both isotopic fractionation and decay between 1950 and year of sample collection (Stuiver and Polach 1977). The error quoted corresponds to the ± 1σ reported by each laboratory, but the actual uncertainty of the

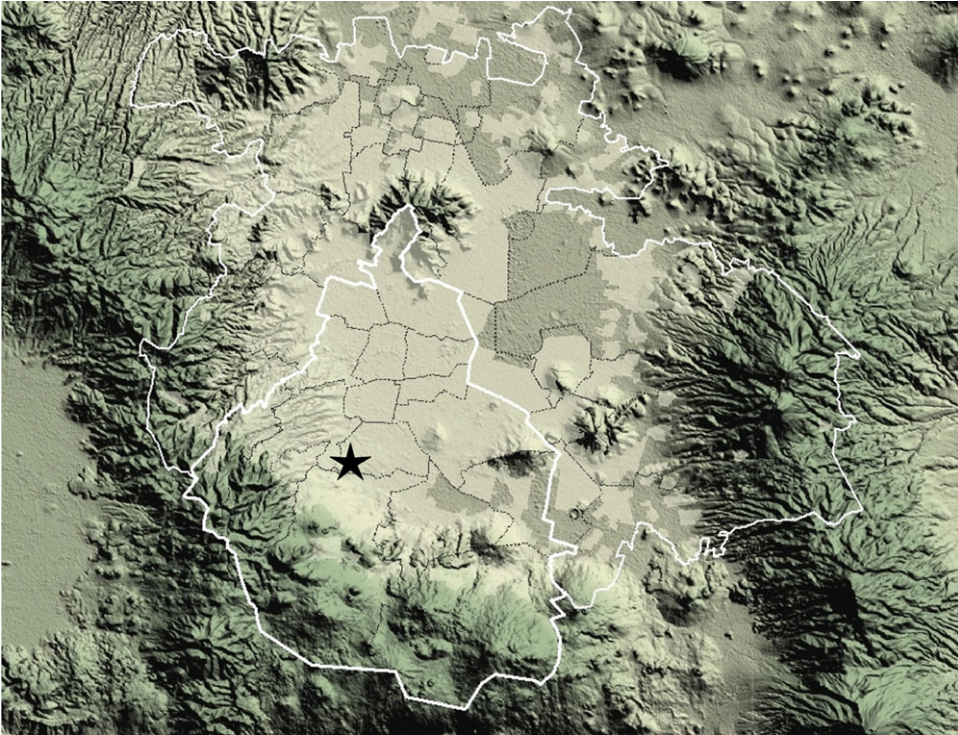


Figure 1 Map of Mexico City and its Metropolitan Area (white line) showing location of sampling point (star). Modified from SEDEMA (<http://www.aire.cdmx.gob.mx/default.php?opc=%27ZaBhnmM=%27>).

data may be higher due to other factors that were not accounted for, such as minor contamination or variability in sample preparation procedures.

RESULTS

Radiocarbon concentrations for integrated CO₂ samples collected in MCMA for the period January 2019–December 2021 are plotted in Figure 2 and tabulated in the supplementary file. Niwot Ridge $\Delta^{14}\text{C}$ preliminary data, considered the regional background values (Lehman and Miller 2019; Lehman et al. 2013), are also plotted for comparison as discussed below.

Comparison with Background $\Delta^{14}\text{C}$ Values

Radiocarbon observations for MCMA are, except for two samples, lower than background values and vary over a wide range from -44.15‰ to 2.25‰ , which appears to be a result from a complex mixture of CO₂ emission sources with different ^{14}C concentration and changes in the volume of fossil fuels consumption in MCMA. All data obtained for samples collected during 2019 and 2021 are significantly lower than data reported for NWR. For the period January–December 2019, values reported for Niwot Ridge range between -7.5‰ (May) and $+7.5\text{‰}$ (August); whereas values found for Mexico City range between -44‰ (December) and -13‰ (October). For 2021, the reported data for NWR cover only up to June with values ranging from -10‰ (May) to -1.5‰ (March), while values for samples from MCMA range from -32.89‰ (November) to -10.27‰ (January-February). On the other hand, $\Delta^{14}\text{C}$ values for

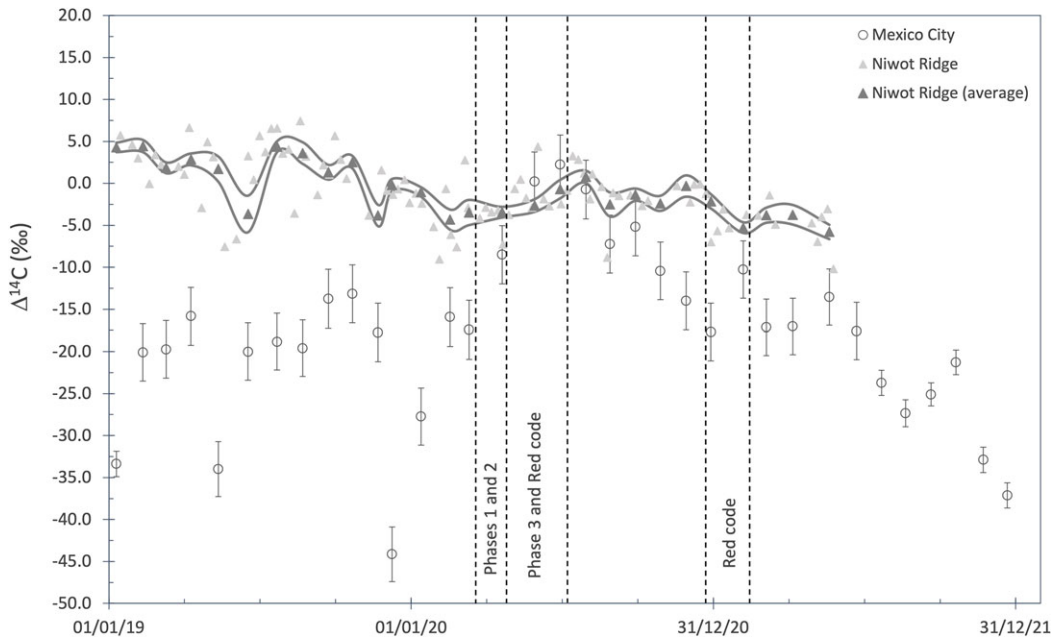


Figure 2 $\Delta^{14}\text{C}$ values for integrated CO_2 samples collected in MCMA (open circles) and for Niwot Ridge as regional background values (gray triangles, data from Lehman and Miller [2019] and Lehman et al. [2013]). Average $\Delta^{14}\text{C}_{\text{NWR}}$ values with the corresponding 95% confidence interval (dark triangles and solid lines) were calculated for estimating the mean background value during the same sampling period in MCMA. Vertical lines mark dates of lockdown phases and red code periods (extremely high epidemic risk).

samples collected in MCMA during the period March–September 2020, when more strict lockdown restrictions were in place, are of the same magnitude as the data reported for Niwot Ridge. For 2020, the NWR values range between -9‰ (February) and 4.5‰ (June) while for MCMA range between -27.74‰ (January) and 2.2‰ (June), with values for May and July of the same order as the background values. This suggests that the increase in atmospheric $^{14}\text{CO}_2$ concentration in MCMA to values similar to those registered at a background site is a result of the significant reduction in fossil fuels consumption associated with the different phases of the lockdown and epidemic risk level during the COVID-19 pandemic in Mexico. To explore this further, the volume of fossil fuels sold for vehicle traffic (gasolines and diesel) reported by the Mexican Petroleum company (PEMEX) is plotted in Figure 3 together with the difference between the background and observed values ($\Delta\Delta^{14}\text{C}_{\text{NWR-MCMA}}$) and the correlation plot comparing both, the $\Delta^{14}\text{C}$ and $\Delta\Delta^{14}\text{C}_{\text{NWR-MCMA}}$ to the volume of fossil fuels. The Pearson correlation coefficient between the sales of fossil fuels and $\Delta^{14}\text{C}$ values is $r=-0.4675$ ($p<0,01$) and a $r=0.7328$ ($p<0.001$) is obtained when comparing against $\Delta\Delta^{14}\text{C}_{\text{NWR-MCMA}}$, confirming the potential of ^{14}C as a tracer of fossil CO_2 in the atmosphere of this complex urban area. Furthermore, the fact that the correlation between $\Delta\Delta^{14}\text{C}_{\text{NWR-MCMA}}$ and fuels use is higher than the correlation between $\Delta^{14}\text{C}$ and fuels use, demonstrates that when the long-term trend is removed by subtracting background, the local impact of fossil fuels on the atmosphere becomes much clearer.

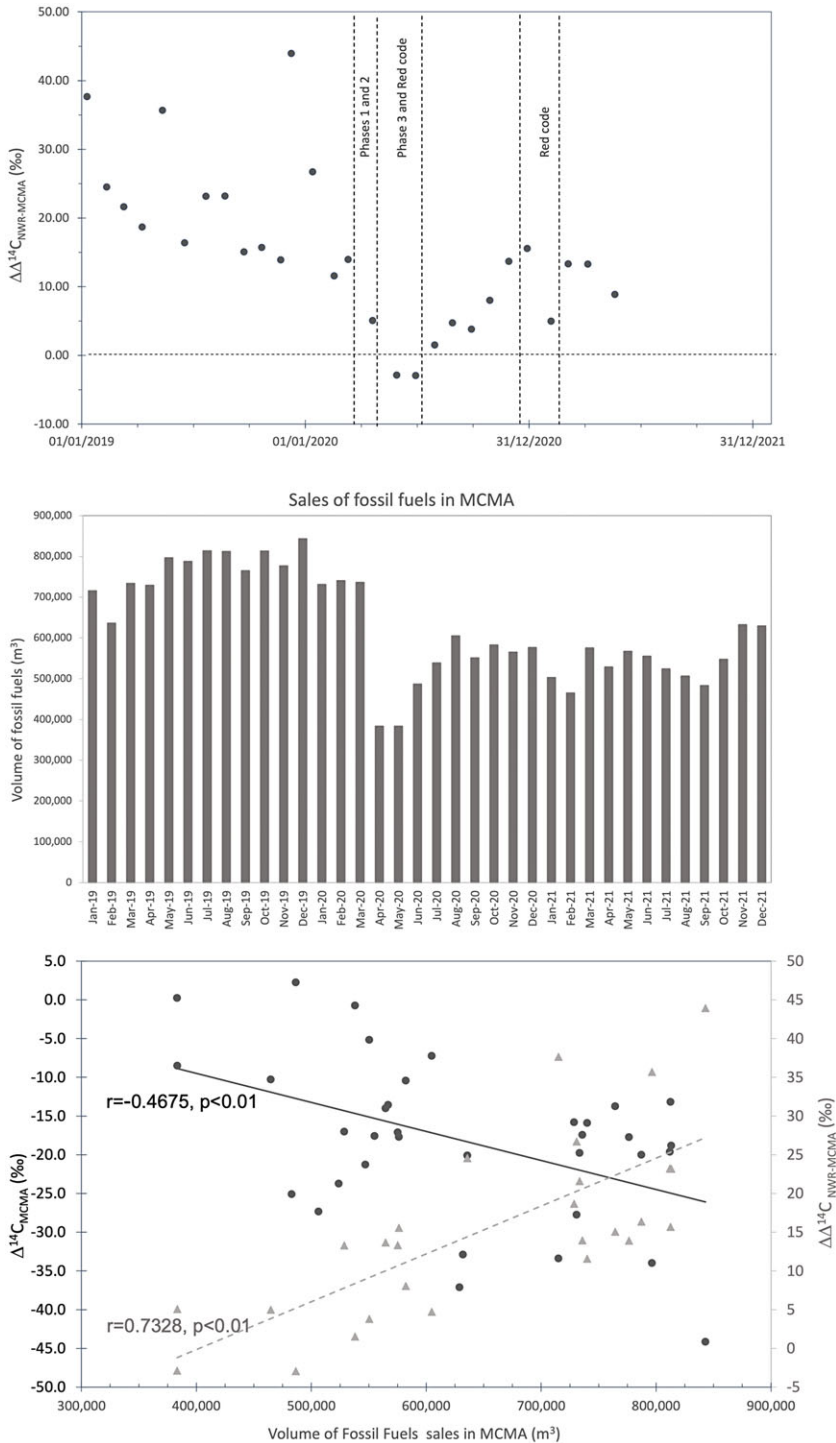


Figure 3 Difference between calculated average background values and observed values ($\Delta\Delta^{14}\text{C}_{\text{NWR-MCMA}}$) with the lockdown phases indicated by vertical lines (top panel). Volume of gasolines and diesel sales in the MCMA (Secretaría de Energía, data taken from <https://sie.energia.gob.mx/bdiController.do?action=cuadro&cvccua=PMXE2C03>) (center panel) and correlation plot comparing the volume of fossil fuels sales to the $\Delta^{14}\text{C}$ (black circles and black solid line) and to the $\Delta\Delta^{14}\text{C}_{\text{NWR-MCMA}}$ (gray triangles and gray dashed line) (bottom panel).

Atmospheric ^{14}C Variations in MCMA during 2019

Samples collected during 2019 have $\Delta^{14}\text{C}$ values ranging between -44.15‰ and -13.17‰ (Figure 2). Higher values were found for samples collected during April, September, and October, although differences are of the same magnitude as the analytical uncertainty reported by the laboratories. On the other hand, significantly lower values were found for samples collected during January, May and December. The dispersion of values confirms the complexity of emission sources in the MCMA previously reported (Beramendi-Orosco et al. 2015, 2018). The apparently higher values found for April may be a result of the ^{14}C -enriched CO_2 released from the numerous forest and agricultural fires around MCMA (Figure 4), whereas higher values found for September and October 2019 seem to be related to the contribution from soils heterotrophic respiration at the end of the rainy season, as during these months the number of fires is low (Figure 4). By contrast, lower values found for May 2019 may be attributed to air stagnation and low ventilation of emissions in the valley during an extraordinary four-days period (14–17 May 2019) when pollution levels were extremely higher than the recommended guidelines. The low values found for January and December 2019 may be related to both, an increase in fossil fuels consumption for domestic combustion during winter, and pollutants accumulation during days with meteorological conditions that promote air stagnation. This is also in accordance with the low number of fires registered around MCMA during these months (Figure 4), suggesting the contribution of ^{14}C -enriched CO_2 from this source is low.

Atmospheric ^{14}C Variations in MCMA during the COVID-19 Pandemic

For samples collected during 2020, $\Delta^{14}\text{C}$ values range between -17.7‰ and $+2.25\text{‰}$ (Figure 2), with a rising trend immediately after the beginning of the lockdown phase 1 (20th March, Table 1), reaching the higher values during the lockdown phases 2 and 3 (April–June). From 1st of July, when the non-essential activities gradually opened according to the epidemic risk level, $\Delta^{14}\text{C}$ values follow a decreasing trend until December 2020. For samples collected during 2021, $\Delta^{14}\text{C}$ values range between -32.89‰ and -10.27‰ ; with a general decreasing trend and apparent peaks for samples collected during January–February, May, and October, although variations are of the same order as the analytical uncertainty, they may be a result of changes in the epidemic risk level, as discussed next.

The $\Delta^{14}\text{C}$ variations seem to be related to changes in fossil CO_2 emissions associated to the different stages of lockdown and epidemic risk (Table 1). First, for April 2020, the number of fires around MCMA registered is similar to those registered during April 2019 (Figure 4); however, the $\Delta^{14}\text{C}$ value obtained for the sample collected during April 2020 is higher, suggesting this could be partly attributed to the $^{14}\text{CO}_2$ emitted by the fires and partly to the decrease in the emission of fossil fuels-derived CO_2 during the lockdown phases 1 and 2. This is in good agreement with the reduction in gasolines and diesel sales in the MCMA, 47% if compared to same month in 2019 (Figure 3). The higher $\Delta^{14}\text{C}$ values were obtained for samples collected between May and June 2020, during the complete lockdown period of phase 3 and extremely high level of epidemic risk, reflecting a significant decrease in fossil CO_2 emissions and in good agreement with the 52% and 38% decrease in fossil fuels consumption in MCMA during May and June, respectively. Interestingly, results for the samples collected during lockdown phases 2 and 3 are also in accordance with the reduction in NO_2 found by Hernández-Paniagua et al. (2021), ranging between 10 and 23% during phase 2 (20 March–21 April) and 43% during phase 3 (21 April–31 May) and attributed to the significant reduction in motor vehicle emissions.

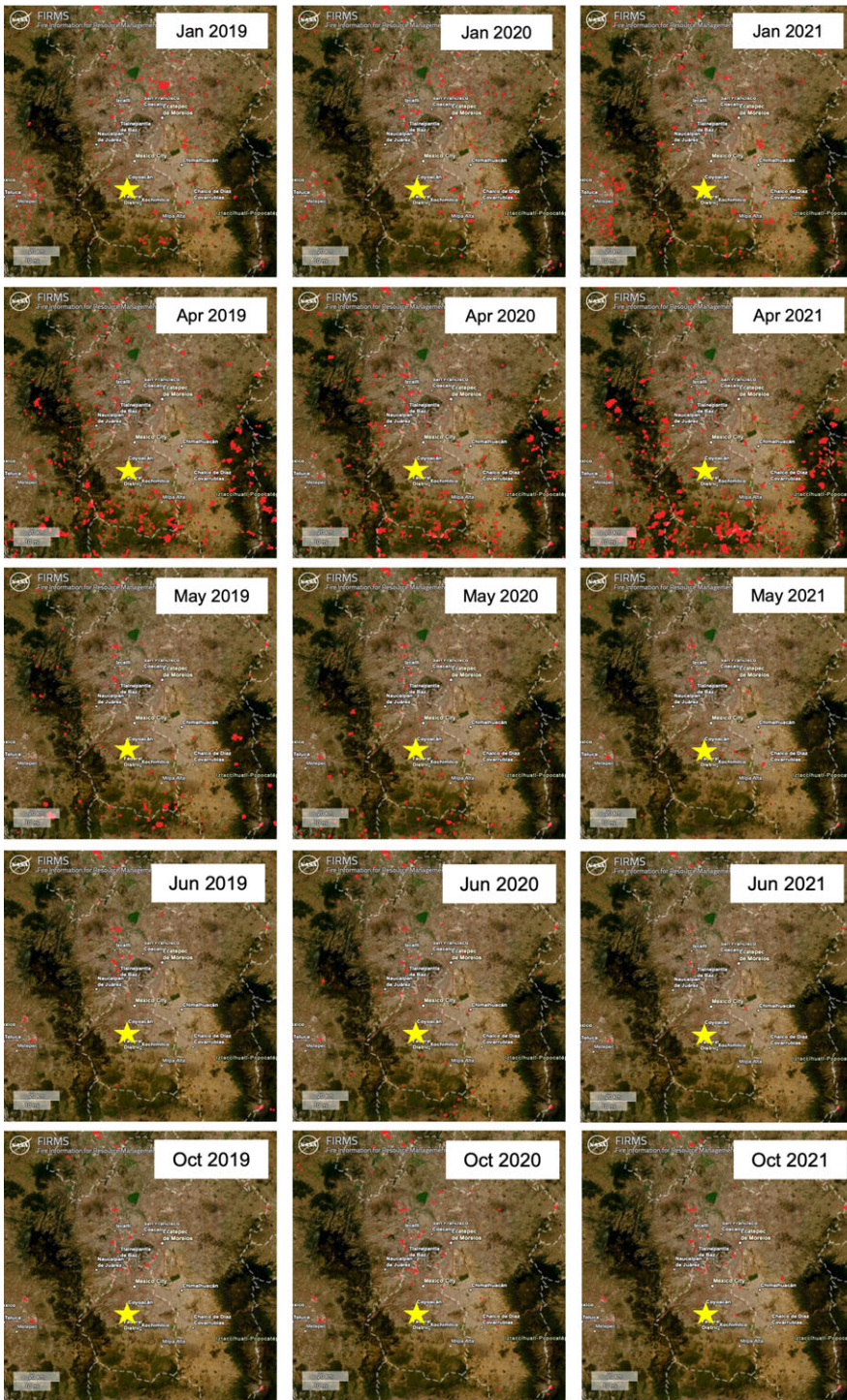


Figure 4 Fires and hot spots registered around the Mexico City Metropolitan Area during some sampling periods. Images taken from NASA’s Fire Information for Resource Management System (FIRMS) available at <https://firms.modaps.eosdis.nasa.gov/>.

From July, the $\Delta^{14}\text{C}$ values follow a decreasing trend, suggesting an increase in fossil CO_2 emissions, also in agreement with the trend in fossil fuels consumption (Figure 3) and the gradual activation of non-essential activities. Furthermore, there is an increase in $\Delta^{14}\text{C}$ for the sample collected during January–February 2021, when the epidemic risk level returned to extremely high (red), with a reduction in fossil fuels consumption of 30% as compared to the volume sold during the same months in 2019 (Figure 3). The low number of fires detected around the MCMA during January 2021 (Figure 4) confirm that the increase in $\Delta^{14}\text{C}$ is not related to the emissions of ^{14}C -enriched CO_2 released by forest and agricultural fires; but seems to be a consequence of the reduction in the fossil CO_2 emissions from the transport sector associated to the restrictions to the non-essential activities. Samples collected between March and June 2021 have $\Delta^{14}\text{C}$ values similar to the values found for samples collected during the same months in 2019, suggesting the fossil fuels consumption is still lower than before the COVID-19 pandemic, in good agreement with fossil fuels consumption (Figure 3). On the other hand, samples collected between July and December 2021 have lower $\Delta^{14}\text{C}$ values than samples collected during the same months in 2019; this should not be interpreted as fossil CO_2 emissions returning to pre-COVID-19 levels, as during these months the fossil fuels consumption was still lower than in 2019 (Figure 3). Although the NWR data do not cover this period, this decreasing trend in $\Delta^{14}\text{C}$ values may be partly explained by the decreasing trend of $\Delta^{14}\text{C}$ concentration in the background atmosphere registered at monitoring stations such as Niwot Ridge, Colorado (Lehman et al. 2013) or Jungfraujoch and other sites from the Heidelberg global network (Levin et al. 2022), resulting from the fossil CO_2 emissions at a global scale.

CONCLUSIONS

We present a record of $\Delta^{14}\text{C}$ values for integrated samples collected in the MCMA during the period January 2019–December 2021. Values found during January 2019–February 2020, before the COVID-19 pandemic, reflect the complexity of emission sources in the area, with fossil fuels combustion as the main CO_2 source, but with other emission sources with high ^{14}C concentration, such as fires during the dry season and heterotrophic respiration during the raining season, resulting in values with significant variations. Despite this complexity, it was possible to identify a change in fossil CO_2 emissions resulting from the COVID-19 lockdown and the restrictions imposed to control transmission of the disease, mainly reflected in a reduction of vehicle traffic, and thus in the consumption of fossil fuels. This is reflected by the variations in $\Delta^{14}\text{C}$ values obtained for samples collected after March 2020, clearly following the chronology of the restrictions imposed to control the spread of the COVID-19 epidemic. These restrictions, which significantly impacted the vehicle traffic, resulted in $\Delta^{14}\text{C}$ values of the same order as the preliminary data for the background atmosphere at Niwot Ridge, confirming the transport sector as the main source of fossil CO_2 and supporting the consideration that other non-fossil CO_2 sources, such as biomass burning and respiration, do contribute to the complexity of emissions in the MCMA.

It is relevant to continue the $^{14}\text{CO}_2$ monitoring programs and work towards a better understanding of the ^{14}C dynamics in the MCMA, which can help to evaluate changes in emission sources and the impact of environmental programs to mitigate the pollution in the area and cut the greenhouse emissions.

ACKNOWLEDGMENTS

This research was funded by DGAPA–UNAM (project PAPIIT-IN109921). Financial support from CONACyT (Consejo Nacional de Ciencia y Tecnología – México) to the Laboratorio Nacional de Geoquímica y Mineralogía is gratefully acknowledged. We are grateful to Scott J. Lehman (INSTAAR, University of Colorado at Boulder) and John B. Miller (NOAA ESRL Global Monitoring Laboratory) who kindly provided NWR data and made constructive suggestions. Finally, comments from two anonymous reviewers helped to significantly improve this manuscript.

SUPPLEMENTARY MATERIAL

To view supplementary material for this article, please visit <https://doi.org/10.1017/RDC.2023.76>

REFERENCES

- Beramendi-Orosco LE, González-Hernández G, Martínez-Jurado A, Martínez-Reyes A, García-Sámamo A, Villanueva-Díaz J, Santos-Arévalo FJ, Gómez-Martínez I, Amador-Muñoz O. 2015. Temporal and spatial variations of atmospheric radiocarbon in the Mexico City Metropolitan Area. *Radiocarbon* 57(3):363–375.
- Beramendi-Orosco LE, González-Hernández G, Martínez-Reyes A, Morton-Bermea O, Santos-Arévalo FJ, Gómez-Martínez I, Villanueva-Díaz J. 2018. Changes in CO₂ emission sources in México City Metropolitan Area deduced from radiocarbon concentrations in tree rings. *Radiocarbon* 60(1):21–34.
- Castillo-Argüero S, Martínez-Orea Y, Romero-Romero MA, Guadarrama-Chávez P, Niñez-Castillo O, Sánchez-Galien I, Meave JA. 2007. La Reserva Ecológica del Pedregal de San Ángel: Aspectos florísticos y ecológicos. México. Universidad Nacional Autónoma de México. pp. 294.
- Hernández-Paniagua IY, Valdez SI, Almanza V, Rivera-Cárdenas C, Grutter M, Stremme W, García-Reynoso A, Ruiz-Suárez LG. 2021. Impact of the COVID-19 lockdown on air quality and resulting public health benefits in the Mexico City Metropolitan Area. *Frontiers in Public Health* 9:642630. doi: [10.3389/fpubh.2021.642630](https://doi.org/10.3389/fpubh.2021.642630)
- INEGI (Instituto Nacional de Estadística y Geografía). Anuario estadístico y geográfico de la zona metropolitana del Valle de México. 2014. Instituto Nacional de Estadística y Geografía. México. 324 p.
- Jauregui E. 2004. Impact of land-use changes on the climate of the Mexico City Region. *Investigaciones Geográficas, Boletín del Instituto de Geografía, UNAM* 55:46–60.
- Lehman SJ, Miller JB. 2019. University of Colorado, Institute of Alpine and Arctic Research (INSTAAR), Radiocarbon Composition of Atmospheric Carbon Dioxide (¹⁴CO₂) from the NOAA ESRL Carbon Cycle Cooperative Global Air Sampling Network, 2003–2018, Version: 2022-12-10. Path: <ftp://ftp.cmdl.noaa.gov/ccg/co2c14/flask/event/>
- Lehman SJ, Miller JB, Wolak C, Southon J, Tans P, Montzka SA, Sweeney C, Andrews A, LaFranchi B, Guilderson TP, Turnbull J. 2013. Allocation of terrestrial carbon sources using ¹⁴CO₂: methods, measurement, and modeling. *Radiocarbon* 55(3):1484–1495.
- Levin I, Hammer S, Kromer B, Preunkert S, Weller R, Worthy DE. 2022. Radiocarbon in global tropospheric Carbon Dioxide. *Radiocarbon* 64(4):781–791. doi: [10.1017/RDC.2021.102](https://doi.org/10.1017/RDC.2021.102)
- Rzedowski GC, Rzedowski J. 2005. Flora fanerogámica del Valle de México. 2nd ed. Instituto de Ecología y Comisión Nacional para el Conocimiento y Uso de la Biodiversidad. 1406 p.
- Secretaría de Salud. 2020. Semáforo de riesgo epidemiológico COVID-19: indicadores y metodología. Available at: https://coronavirus.gob.mx/wp-content/uploads/2020/06/Lineamiento_Semaforo_COVID_05Jun2020_1600.pdf. Accessed January 2023.
- SEDEMA (Secretaría del Medio Ambiente Ciudad de México). 2021. Inventario de Emisiones de la Zona Metropolitana del Valle de México 2018. Available at: <http://www.aire.cdmx.gob.mx/default.php?opc=Z6BhnmI=&dc=Zg>=>. Accessed January 2023.
- SENER (Secretaría de Energía México). 2022. Sistema de Información Energética. Available at: <https://sie.energia.gob.mx/bdiController.do?action=cuadro&cvecuca=PMXE2C03>. Accessed January 2023.
- Stuiver M, Pollach H. 1977. Discussion: Reporting of ¹⁴C data. *Radiocarbon* 19(3):355–363.
- Vay SA, Tyler SC, Choi Y, Blake DR, Blake NJ, Sachse GW, Diskin GS, Singh HB. 2009. Sources and transport of ¹⁴C in CO₂ within the Mexico City Basin and vicinity. *Atmospheric Chemistry and Physics* 9:4973–4985.